Journal of Catalysis **210,** 285–294 (2002)
doi:10.1006/jcat.2002.3677

Pd-Modified Cu–Zn Catalysts for Methanol Synthesis from CO_2/H_2 Mixtures: Catalytic Structures and Performance

I. Melián-Cabrera, M. López Granados, and J. L. G. Fierro[1]

Instituto de Catálisis y Petroleoquímica, Consejo Superior de Investigaciones Científicas, Campus Cantoblanco, 28049 Madrid, Spain

Received December 14, 2001; revised March 15, 2002; accepted May 8, 2002

The effect of palladium incorporation on the performance of a CuO–ZnO catalyst for methanol synthesis by hydrogenation of carbon dioxide is studied. Three different catalysts are prepared: the reference CuO-ZnO (CZ), and two Pd-based CuO–ZnO catalysts, PCZ-CP and PCZ-SP, which are prepared by co-precipitation and sequential precipitation, respectively. The PCZ-CP system appears to be almost inactive for methanol synthesis, whereas the PCZ-SP catalyst increases the methanol yield [mol MeOH/(h kg_{cat})] with respect to the base CZ catalyst. The marked decrease in the catalytic activity of the PCZ-CP catalyst is explained in terms of the loss in copper surface area. The effect of Pd is not capable of overcoming this significant loss in copper surface area. The enhanced methanol yield for PCZ-SP is not due to additional active palladium sites, but to a synergetic effect of Pd on the active Cu sites. The increase in the amount of hydrogen consumed (H_2/M) during copper oxide reduction for PCZ-SP suggests that an H_2-spillover mechanism is responsible for the increase in the methanol yield. This research reveals the importance of the methodology used for the incorporation of palladium. The results show that the precipitation order has a remarkable influence on the properties of the active phases and, consequently, on the catalytic performance for the hydrogenation of CO_2 to methanol.

Key Words: **carbon dioxide hydrogenation; methanol synthesis; hydroxycarbonate precursors; Pd-modified catalysts; TPR; H_2 spillover; promoting effect; structure–activity relationship.**

1. INTRODUCTION

Methanol is conventionally produced from synthesis gas (a mixture of $CO/CO_2/H_2$) derived from natural gas over a ternary $CuO–ZnO–Al_2O_3$ catalyst at 50–100 bar and 473–523 K (1). Recent studies of CO_2 hydrogenation have received much attention, drawing interest to the role of CO_2 in the industrial methanol-synthesis conditions. Kinetic experiments, using isotope-labelled carbon oxides (2, 3) and spectroscopic experiments (4), have demonstrated that under industrial conditions methanol is produced by hydrogenation of CO_2, where CO merely provides a source of CO_2 and acts as a reducing agent. Nevertheless, the ternary Cu–Zn–Al catalyst is not as active for CO_2-rich reaction mixtures (5, 6).

Within this frame, the conventional catalyst has been modified in order to improve the catalytic performance for methanol synthesis from H_2/CO_2 feeds. The CuO–ZnO catalysts have been widely modified with different metals such as chromium (7), zirconium (8–10), vanadium (10), cerium (11), titanium (12, 13), gallium (14, 15), and palladium (16–20).

We recently investigated the promotional effect of Pd on a Cu–Zn–Al oxide catalyst for the hydrogenation of CO_2 (21). We found that wet palladium impregnation causes a dramatic decrease of the methanol yield, and this was explained in term of genesis, decomposition, and reconstruction of hydrotalcite-like precursor structures. In addition, there is still a lack of agreement on the optimum method for preparing palladium-containing catalysts supported on different oxides. The discrepancies found could be due to the use of a preparation method that is not fully reproducible and may give rise to a nonhomogeneous distribution of the palladium particles on the surface (22).

In order to circumvent the serious drawbacks of aqueous impregnation of *ex* hydrotalcite mixed oxides, we made an extensive study of other methods such as precipitating procedures. Precipitation may be a suitable procedure to add noble metals to conventional heterogeneous catalysts (23, 24), allowing homogeneous distribution of the precious metal inside the precursor, which by further calcination can give rise to highly dispersed metal particles.

This continuing research begins with the modification of the model CuO–ZnO methanol synthesis catalyst by different precipitating procedures. This simpler binary system may provide useful information about the optimal palladium incorporation method, which is extrapolated later to the more complex industrial $CuO–ZnO–Al_2O_3$ system.

In a previous publication we reported a detailed characterisation of Pd-modified Cu–Zn precursors (25). One of the major observations was that the methodology for the incorporation of palladium has a marked effect on the nature of the resulting precursors. Consequently, it is expected that the thermal decomposition in air of these precursors will change the nature of the final oxidic phases.

[1] To whom correspondence should be addressed. Fax: 34 91 585 4760. E-mail: jlgfierro@icp.csic.es.

0021-9517/02 $35.00

The purpose of this continuing work is to present a thorough investigation of the structural and surface properties of the oxidic phases in the final catalysts, and to assess their impact on the performance for the hydrogenation of CO_2 to methanol. The information obtained by the characterisation techniques allows a discussion regarding the structure–activity relationship.

2. EXPERIMENTAL

2.1. Catalyst Preparation

General agreement exists regarding the optimal composition for CuO–ZnO methanol-synthesis catalysts. As reported by Herman *et al.* (26), a catalyst with a CuO–ZnO ratio of 30/70 (wt%) gives rise to the highest methanol yield. Therefore, a reference copper–zinc (CZ) catalyst was prepared with a nominal composition of CuO/ZnO = 30/70 (wt%). Since differences in the preparation conditions (concentrations, pH, temperature, etc.) could result in significantly different precursor structures (27), the conditions were properly and carefully adjusted. The CZ precursor was prepared by co-precipitation of the corresponding metal nitrates at constant pH (ca. 7.0) and constant temperature (323 K) with sodium carbonate. A series of palladium–copper–zinc (PCZ) catalysts, with a nominal composition of PdO–CuO–ZnO = 2/28/70 (wt%), were prepared by two methods: (i) co-precipitation of all the cations (PCZ-CP) and (ii) sequential precipitation (PCZ-SP). In the sequential precipitation (SP), palladium was first hydrolysed in the vessel containing the metal nitrates. Subsequently, the co-precipitation of Cu and Zn cations was carried out in a manner similar to the CZ sample. A detailed description of the catalyst preparation is given elsewhere (28). All the precipitates were aged (323 K for 4 h) under stirring, washed with deionized water to remove residual sodium (less than 0.5 ppm in mother liquid), and dried overnight at 393 K. The catalysts were obtained by calcination of the precursors in air at 623 K. The catalyst powders were pelletized and sieved (0.4–0.5 mm) for characterisation and subsequent use in catalytic experiments. The reproducibility in the preparation of the precursors and catalysts was assured by preparing several batches of each catalyst. The experimental results (characterisation and activity measurements) were quite similar.

2.2. Catalyst Characterisation

The chemical composition (Pd, Cu, and Na) of the calcined catalyst was determined by means of inductively coupled plasma atomic emission spectroscopy (ICP-AES), using a Perkin-Elmer Optima 3300 DV apparatus. Powder X-ray diffraction patterns of calcined catalysts were recorded on a computerised Seifert 3000 XRD diffractometer using Cu $K\alpha$ radiation in the step mode (0.02°, 2 s) in the range $25° < 2\theta < 75°$. The specific area of each calcined sample was calculated by the BET method from the N_2 adsorption isotherms (77 K), which were acquired using a Micromeritics TriStar apparatus. Temperature-programmed reduction (TPR) experiments were carried out in a semiautomatic Micromeritics TPD/TPR 2900 apparatus. The TPR profiles were characterised by three parameters: (i) the temperature at which maximum H_2 consumption was observed (T_M), (ii) the full width at half maximum (FWHM), and (iii) the ratio between the amount of H_2 consumed and the amount of reducible metal species present (H_2/M). For the sake of comparison, the patterns for pure CuO and PdO (Aldrich) reference compounds were also measured. X-ray photoelectron spectra (XPS) were acquired with a VG Escalab 200R spectrometer equipped with a hemispherical electron analyser and Al $K\alpha$ ($h\nu = 1486.6$ eV) X-ray source.

The experimental details and procedures followed with these characterisation techniques were addressed in previous contributions (21, 25).

The amount of exposed copper was measured using a nitrous oxide chemisorption method similar to that described by Chinchen *et al.* (29) called reactive frontal chromatography (RFC). Once the catalyst was reduced in an H_2/N_2 mixture at 513 K for 2 h, it was exposed to a flow of N_2 and cooled to the chemisorption temperature (333 K). A flow of 3 vol% N_2O/N_2 gas mixture was fed into the reactor by switching a four-port valve. The delayed N_2O front produced by the decomposition of N_2O on the exposed Cu atoms (reaction [1]) was monitored using a thermal conductivity detector.

$$2Cu_{(S)} + N_2O_{(g)} \rightarrow Cu_2O_{(S)} + N_{2(g)} \qquad [1]$$

The amount of exposed copper (mole Cu/g_{cat}) was calculated considering a molar stoichiometry of $N_2O/Cu_{(S)} = 0.5$ (i.e., complete coverage of copper via reaction [1]). The copper surface area was also calculated assuming a value of 1.46×10^{19} Cu atoms/m^2 (30) for the copper surface-atom density. The copper metal area of the catalysts was also measured after activity runs. The procedure basically included depressurisation, displacement of the reaction mixture (H_2/CO_2) from the reactor with a flow of N_2, and subsequent cooling to near ambient temperature. Prereduction with an H_2/N_2 mixture and reevaluation of the copper surface area allowed the extent of sintering during reaction to be assessed.

2.3. Catalytic Activity

The catalytic hydrogenation of CO_2 was carried out in a high-pressure stainless-steel fixed-bed tubular reactor by feeding a reaction mixture of H_2 and CO_2 in the molar ratio of $CO_2/H_2 = 1:3$. Prior to the activity measurements, the samples were reduced *in situ* at 513 K (at a heating rate of 5 K/min) with 60 mL/min of a 10 vol% H_2/N_2 mixture for 2 h. The reaction was performed at 60 bar overall pressure and with a W/F value of 0.0675 kg h/m^3. Activity was

measured between 453 and 513 K, running from the lowest to the highest temperature and maintaining the reaction for 4 h at each temperature. The effluents from the reactor were analysed using a Hewlett–Packard 5890 Series II gas chromatograph connected online to the reactor. The steady-state values for CO_2 conversion are quoted as the average of five different analyses taken after 4 h onstream operation at a given temperature.

The experimental details about the configuration of the catalytic bed and other features are given in a previous contribution (21).

3. RESULTS

Previous characterisation results (25) showed that the CZ and PCZ-SP precursors contain a Cu–Zn aurichalcite phase. This mineral occurs naturally, as well as synthetically, as a precursor in the preparation of catalysts for industrial methanol synthesis (26). The PCZ-CP precursor consisted of independent Cu and Zn phases, i.e., sodium–zinc carbonate and an amorphous copper hydroxycarbonate. These results, as summarised in Table 1, are taken into account during the discussion of the current results.

In summary, the findings established in our previous work (25) reveal that the structure of the Pd-modified precursors depends on the preparation conditions used during synthesis. The genesis and growth of the precursors are explained by means of Shen's initial-stage precursor mechanism (28) and the effect of sodium concentration as a kinetic factor. The higher Na^+ concentration that is used for the PCZ-CP material counteracts the formation of a mixed aurichalcite, and gives rise to the formation of independent Cu and Zn phases in the final precursor. For more detailed information regarding the characterisation of the precursors, the reader is referred to Ref. (25).

All the precursors were calcined in air at 623 K (at a heating rate of 10 K/min). The calcination temperature was selected on the basis of the thermogravimetric analysis (TGA) and evolved-gas analysis (EGA) experiments (25). Higher calcination temperatures, which are required for complete decomposition of these precursors, were not used as they are close to the higher limit to avoid thermal sintering of the CuO phase and, therefore, would have an adverse effect on the catalytic activity for methanol synthesis.

TABLE 1

Effect of the Precursor Structure on the Particle Sizes for the Oxidic CuO and ZnO Phases Present in the Catalysts

Sample	Precursor	*D* (crystal size, nm)	
		CuO	ZnO
CZ	Au	9.3	13.0
PCZ-CP	Am–SZC	15.7	26.2
PCZ-SP	Au	9.6	14.3

Note. Precursor phases present: Au, aurichalcite = $(Cu,Zn)_5(CO_3)_2(OH)_6$; Am, amorphous copper hydroxycarbonate = $Cu_2(OH)_{2.54}(CO_3)_{0.73}$; and SZC, sodium–zinc carbonate = $Na_2Zn_3(CO_3)_4 \cdot 3H_2O$. Taken from Ref. (25).

TABLE 2

Chemical Composition (Pd, Cu, and Na) and BET Specific Area of Calcined Catalysts

Catalyst	Chemical composition (wt%)[a]			S_{BET} (m^2/g)
	Pd	Cu	Na	
CZ	—	22.0	0.02	20.4
	(0)	(24.0)	(0)	
PCZ-CP	1.0	17.0	4.80	12.4
	(1.7)	(22.4)	(0)	
PCZ-SP	1.3	19.4	—	24.6
	(1.7)	(22.4)	(0)	

[a] Values in parentheses represent nominal composition (wt%). The symbol (—) indicates values that are under the detection limit of the ICP-AES technique.

3.1. Chemical Analysis

The results of the chemical analyses (Pd, Cu, and Na) of the calcined catalysts, as determined by ICP-AES, are given in Table 2. Nominal compositions of CZ and PCZ catalysts are also included for comparison purposes. The Pd and Cu contents were below the nominal values for all samples. In the cases of CZ and PCZ-SP, the reason for this discrepancy is that some carbonates were still present in the calcined samples subjected to chemical analysis. TGA–EGA spectra of the catalyst precursors showed that, at 623 K, the initial precursor was transformed into a modified oxycarbonate of the type $[Cu,Zn]O_x(CO_3)_{1-x}$ (25). Irrespective of the value of x, the remaining CO_3^{2-} groups had a diluting effect on the calcined samples that resulted in lower metal concentrations with respect to the nominal ones. The Pd and Cu contents of the PCZ-CP catalyst were also lower than expected. Although TGA–EGA experiments showed complete decomposition of the precursor at 623 K (25), a certain proportion of Na (4.38 wt% as Na_2O), arising from decomposition of the crystalline sodium–zinc carbonate phase $[Na_2Zn_3(CO_3)_4 \cdot 3H_2O]$, is present in the calcined catalyst and has a diluting effect on all other elements.

3.2. X-ray Diffraction Analysis of Calcined Catalysts

The interpretation of the XRD patterns of the calcined catalysts was done previously (25). In summary, the calcined materials derived from the aurichalcite precursor decomposition (CZ and PCZ-SP) display smaller CuO and ZnO particle sizes than those obtained from independent copper and zinc precursor phases (PCZ-CP) (Table 1). The latter situation inhibits the interaction between CuO and ZnO during calcination, and leads to large particles of both

oxidic phases. In contrast, the decomposition of the aurichalcite, a mixed Cu–Zn hydroxycarbonate where Cu and Zn atoms are alternately located within the structure, results in smaller crystal dimensions for both CuO and ZnO phases as a consequence of the better interdispersion of such phases upon calcination.

In addition, an important factor to bear in mind is the high Na content in the PCZ-CP catalyst, as revealed by chemical analysis. Jun *et al.* (31) pointed out that residual Na inhibits the interaction between CuO and ZnO phases, leading to poorer Cu dispersion and causing a marked decrease in the efficiency of methanol synthesis by the hydrogenation of CO_2. Therefore, the high loading of residual Na in our PCZ-CP catalyst (ca. 5%) has a detrimental effect on the interaction between the oxidic phases and contributes to the decrease in CuO dispersion.

The BET specific areas of the calcined samples, also given in Table 2, are consistent with the XRD trends. The BET area for the PCZ-CP catalyst is almost half that obtained for the CZ and PCZ-SP samples. This low area is a consequence of the formation of large CuO and ZnO particles produced by thermal decomposition of the PCZ-CP precursor. The CZ and PCZ-SP samples, resulting from the decomposition of the auricalcite precursor, present better-dispersed oxidic phases and hence higher surface areas.

3.3. TPR of the Catalysts

The TPR profiles of the calcined samples, along with those of pure CuO and PdO as reference compounds, are given in Fig. 1. Palladium oxide was reduced isothermally at room temperature (296 K), meaning that the representation of the hydrogen uptake as a function of temperature gave a vertical line. For this reason, it was necessary to plot the hydrogen uptake against time (bottom curve in Fig. 1). The values for the parameter P and the results derived from the TPR experiments are shown in Table 3. The experimental conditions were selected in such a way that the characteristic parameter P lay between the values recommended in the literature. This parameter should be as low as possible within the experimental sensitivity and, in any case, lower than 20 K (32). An inappropriate selection of the experimental conditions would distort the TPR profile and make it unreliable. The experiments were performed with a P value of around 2 K.

The TPR profile of the calcined CZ sample shows only one reduction peak, at around 456 K, which was assigned to the reduction of CuO to Cu: $CuO + H_2 \rightarrow Cu + H_2O$. Although the reduction of zinc oxide is thermodynamically feasible at high temperatures, ZnO was not reduced under the experimental conditions described here. The presence of only one peak in the TPR profile of CZ is in accordance with the literature data, although the temperature of maximum H_2 consumption is different from the temperatures

TABLE 3

Summary of TPR Data for Calcined Samples with Reference Compounds

Catalyst	P (K)	T_M (K)	FWHM (K)[a]	H_2/M[b]	$E_{ACT.}$ (kJ/mol)[c]
CZ	1.9	456	17.5	1.36	53.3 ± 2.6
PCZ-CP	1.5	310–352		1.56	52.1 ± 1.9
		451	33.6 (451)		
PCZ-SP	1.7	345		1.64	49.5 ± 3.1
		441	17.6 (441)		
CuO (Ref)	1.4	544	35.0	Reference	ND[d]
PdO (Ref)	1.4	296–340	ND[d]	Reference	—

[a] Full width at half maximum of the main peak. The value in parentheses is the temperature of the main peak.
[b] The experimental error coinciding with the consumed H_2 was ±5%.
[c] Activation energy for the reduction of CuO.
[d] Not determined.

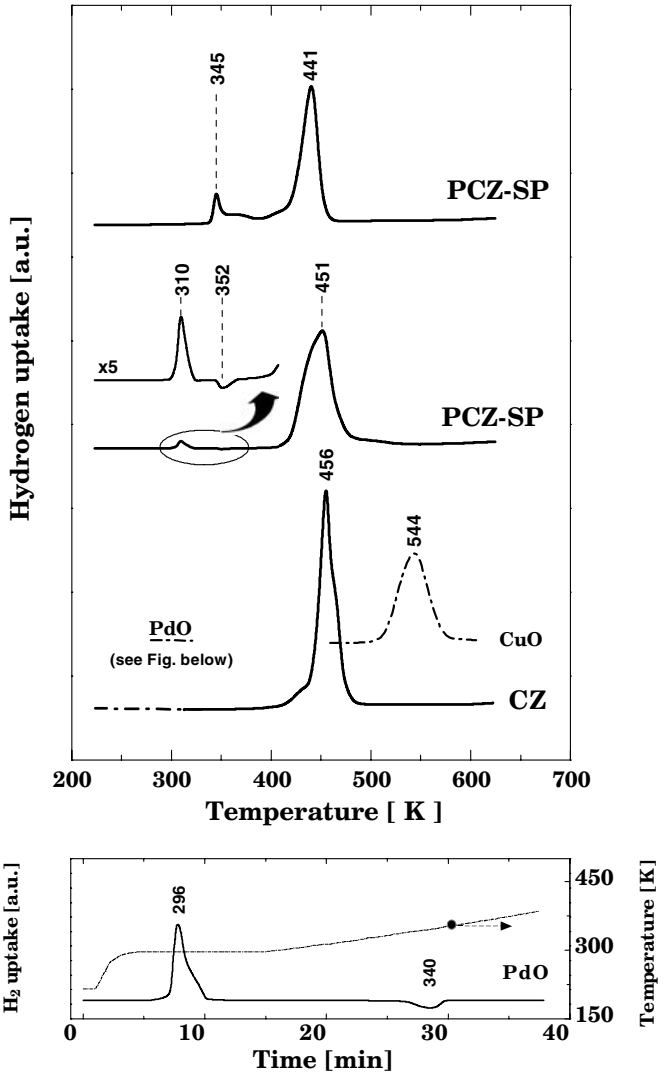

FIG. 1. TPR profiles for calcined samples with those of pure CuO and PdO as reference compounds.

reported previously (32–34). The peak for the CuO reduction of the CZ catalyst was displaced by almost 90 K towards lower temperatures in comparison to that of the CuO reference compound. This result indicates that the presence of ZnO enhances the reducibility of the copper oxide phase in CuO–ZnO catalysts, and this fact agrees with previous observations (32).

The ratio between the amount of hydrogen consumed and the amount of reducible species (Cu^{2+} and Pd^{2+}) present (H_2/M in Table 3) was determined quantitatively. The difference between the experimental and theoretical values, $(H_2/M)_{EXP} = 1.36$ and $(H_2/M)_{THEOR} = 1.00$, is too high to be ascribed to the experimental error inherent in the technique (up to 10%). However, it is known that ZnO is capable of occluding large amounts of hydrogen both on the surface and in subsurface regions (35, 36). The following mechanism is suggested to explain the high $(H_2/M)_{EXP}$ value. At the beginning of the reduction process the formation and growth of metallic Cu particles takes place. Hydrogen is activated on the copper metal and migrates towards the ZnO phase, where it is both adsorbed on the surface and stored in the ZnO crystalline structure. This additional amount of hydrogen, whether adsorbed on the surface or stored in the crystalline ZnO structure, could explain the increase in the $(H_2/M)_{EXP}$ value found for the CZ sample. This explanation is also valid for Pd-containing samples, although these systems behave in a special way: even more hydrogen is taken up than for the CZ sample, a phenomenon that will be discussed in following text.

The TPR experiments on the Pd-containing catalysts were carried out after cooling the samples down to cryogenic temperatures (ca. 223 K), since PdO is reduced at low temperatures. Two different regions can be distinguished in the TPR profile of the PCZ-CP catalyst (Fig. 1). The first region includes a reduction peak close to ambient temperature (310 K) and a desorption peak at 352 K. The second region consists of a broad reduction peak at 451 K. The first region, in comparison with the profile of the PdO reference compound (bottom curve in Fig. 1), can be assigned to the reduction of large, isolated PdO particles to Pd and the formation of a hydride species (PdH_X) that decomposes at higher temperature (negative peak in the TPR profile). This interpretation is also consistent with the results obtained by Chang *et al.* in a study of Pd–ZnO systems (37). In addition, the hydrogen consumed at the low temperature peak (310 K), after subtraction of the amount of hydrogen released in the subsequent desorption peak, corresponds to the stoichiometric amount required for the complete reduction of PdO. The second region is attributed to the reduction of CuO. It should be noted that the peak width (i.e., FWHM in Table 3) for this region is higher than that for the CZ catalyst, but the positions of the peak maxima are almost identical. These observations lead us to believe that the CuO species in both catalysts show the same reducibility at the beginning of the reduction process but the PCZ-CP sample requires longer time for the reduction to be completed. This retardation effect is explained in terms of intraparticle mass transfer limitations (32) because of the marked difference between the CuO crystal sizes in the two catalysts (see Table 2).

The PCZ-SP catalyst showed two peaks at 345 and 441 K. On comparing this profile with that obtained for PCZ-CP, it is seen that the reduction peak at 310 K, attributed to isolated PdO phases, does not appear in the SP case. This indicates that the PdO phase is well dispersed and interacting with the Cu–Zn bulk oxides, making the reduction of PdO more difficult. The H_2 consumption at 345 K not only corresponds to palladium oxide reduction ($PdO + H_2 \rightarrow Pd + H_2O$) but also to partial Cu^{2+} reduction. This situation is deduced by the fact that the H_2 consumption exceeds the stoichiometric amount of H_2 required for the complete reduction of PdO (nearly ninefold higher). Additional evidence for the partial reduction of Cu^{2+} will be discussed in more detail in the XPS section. The second peak at 441 K, which is shifted slightly but clearly towards lower temperatures with respect to the CZ catalyst, corresponds to the reduction of the remaining CuO to Cu metal. These features of CuO reduction, i.e., partial reduction of CuO at low temperatures and the shift of the main CuO reduction peak towards lower temperatures, point to some kind of promoting effect of palladium metal on the reducibility of Cu^{2+}. This promoting effect could be caused by either a decrease in the activation energy of the rate-determining step or by an increase of the pre-exponential term in the Arrhenius equation (38). In order to understand this aspect in more detail, the activation energy of the CuO reduction was determined by means of the Kissinger method (39). This method predicts that a plot of $\ln(\beta/T_M^2)$ vs. $1/T_M$ gives a straight line with a slope of $-E_{ACT}/R$, where β is the heating rate and T_M is the temperature at the peak maximum. As an example, Fig. 2 shows the profiles obtained for different heating rates (part A) and the Kissinger plot (part B) for CuO reduction in the CZ sample.

The values obtained for the activation energies are given in Table 3. The values for the systems CZ and PCZ-SP, 53.3 and 49.5 kJ/mol respectively, do not differ significantly and agree with the data reported by Gentry *et al.* (40). These authors studied the influence of metal additives on the reducibility of CuO, and did not find any influence of palladium on the activation energy of CuO reduction. As a consequence, the effect of palladium on the reducibility of CuO, in our PCZ-SP catalytic system, seems to be a result of an increase in the pre-exponential factor. The fact that the palladium sites are reduced at a lower temperature than the copper sites, together with the ability of Pd to activate the H_2 molecule, leads us to believe that this metal is performing its function of enhancing the CuO reducibility in two ways: (i) increasing directly the number of nucleation

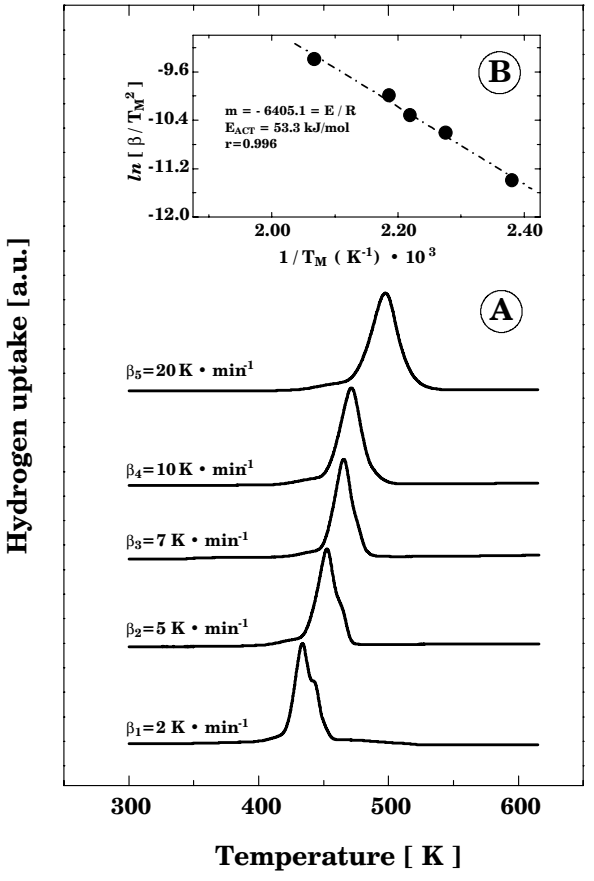

FIG. 2. TPR profiles for CuO reduction in the CZ catalyst (A) at different heating rates and (B) Kissinger plot.

centers by creating new palladium-rich reduction centers and/or (ii) providing a high concentration of active hydrogen that is susceptible for use in CuO reduction. Whatever pure or combined mechanism is functioning, the reduction of CuO is facilitated. From the experimental data, the second hypothesis appears more likely since the H_2/M ratios of the Pd-containing catalysts are higher than those of the CZ counterpart. Hydrogen is easily dissociated on Pd particles and then spills over to the Cu–ZnO phase.

3.4. X-ray Photoelectron Spectroscopy

Photoelectron spectroscopy was used to evaluate the oxidation state of copper species during the low-temperature reduction process of the PCZ-SP catalyst. For this purpose, the spectra of both the outgassed calcined catalyst and the H_2-reduced catalyst were recorded; their Cu $2p_{3/2}$ core-level spectra are displayed in Fig. 3. The calcined and outgassed sample (Fig. 3, part A) displays the main Cu $2p_{3/2}$ peak somewhat above 934 eV, which is characteristic of Cu^{2+} species (41, 42). The high value of the FWHM for the Cu $2p_{3/2}$ level in the calcined sample and its asymmetry towards higher binding energies suggest that the Cu $2p_{3/2}$ peak could consist of more than one contribution. On this basis, the peak profile was deconvoluted into two contributions centered around 934.6 and 937.1 eV. The peak at 937.1 eV is assigned to a copper–CO_3^{2-} bond in which the CO_3^{2-} anions remaining in the calcined sample could be responsible for this chemical shift. The peak at 934.6 eV is attributed to Cu^{2+} in a CuO-like environment. Additional evidence for the presence of Cu^{2+} ions is provided by the satellite structure (Cu^{2+}_{SAT} in Fig. 3, part A) caused by electron shake-up processes. The satellite area-intensity relative to the main peak (I_S/I_M) of 0.61 for the Cu $2p_{3/2}$ band is in good agreement with the values for the CuO–ZnO mixed oxides reported by Okamoto *et al.* (41).

H_2 reduction at 373 K changes the Cu $2p_{3/2}$ line profile considerably (Fig. 3, part B). The significant decrease in the satellite peak ($I_S/I_M = 0.20$) and the simultaneous shift of the main Cu $2p_{3/2}$ peak towards lower binding energies are a consequence of the reduction of surface Cu^{2+} to lower oxidation states, i.e., Cu^+ or Cu^0. The profile consists of a principal peak at 932.6 eV, assigned to reduced Cu^+/Cu^0 species, and a smaller one centered at 934.6 eV, which is attributed to Cu^{2+} in a CuO environment and indicates that some copper is still oxidised. Differentiation between reduced

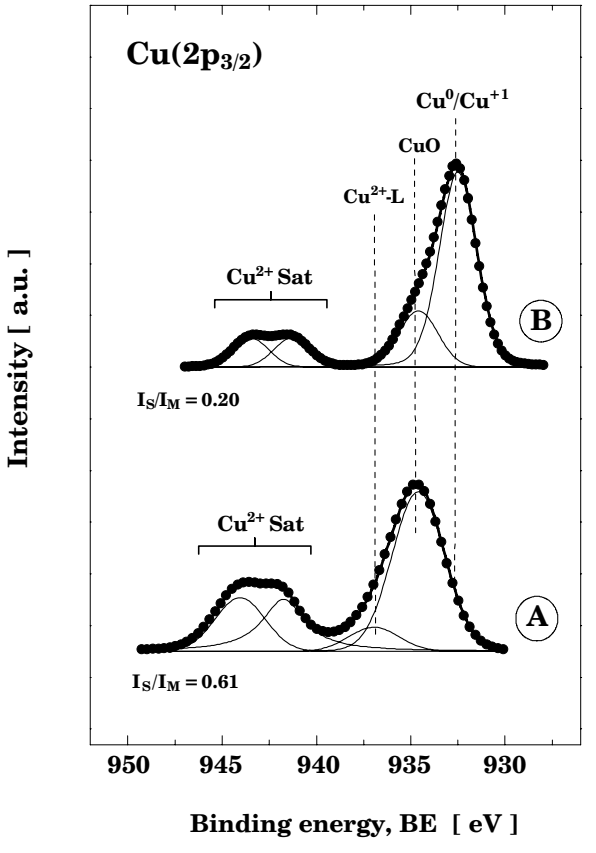

FIG. 3. Cu $2p_{3/2}$ core-level spectra for (A) outgassed and (B) H_2-reduced PCZ-SP catalyst. The reduction was performed at 373 K in the pretreatment chamber of the spectrometer.

Cu^+ and Cu^0 species at 932.6 eV is impossible on the basis of binding energy analysis alone. The distinction between these species is only feasible through examination of the modified Auger parameter (43). The modified Auger parameter, defined as $\alpha_{A'} = h\nu + [Cu(L_3VV) - KE\ Cu\ 2p_{3/2}]$, represents the difference between the kinetic energy of the $Cu(L_3VV)$ Auger electron and the $Cu\ 2p_{3/2}$ photoelectron. Addition of the energy of the incident photon ($h\nu$) allows the modified Auger parameter to be independent of the excitation energy. A value of 1850.8 eV for the species with a binding energy of 932.6 eV indicates the presence of Cu^0 (44).

These results constitute direct evidence that the low-temperature reduction process in the TPR experiment for the PCZ-SP sample involves the simultaneous reduction of all PdO as well as the reduction of almost all surface CuO to Cu^0 metal. The XPS technique clearly shows the influence of palladium metal on the reduction of CuO.

3.5. Copper Surface Area of Fresh and Postreaction Catalysts

The copper surface area was determined by means of N_2O chemisorption, and gave an indication of the amount of Cu^0 exposed to the reactants. This is an important parameter for Cu-based catalysts, particularly for methanol-synthesis catalysts. Nevertheless, the interference by palladium in the determination of exposed copper should not be neglected. Palladium can react with an N_2O probe molecule, as already suggested in a previous contribution (21). As a consequence, care must be taken with the information provided by this technique. The true amount of exposed copper for the modified catalysts must be lower than estimated by this technique, and this fact has to be considered in the discussion of the present results.

The amount of exposed copper for the fresh reduced catalysts is given in Table 4 (first column). It is observed that the values for the CZ and PCZ-SP catalysts are similar, while the PCZ-CP system displays a value about 60% lower for the exposed copper.

TABLE 4

N_2O Chemisorption Data for Fresh and Postreaction Catalysts

	Fresh catalysts		Postreaction
Catalyst	Exposed copper[a] (μmol Cu_S/g_{cat})	Cu dispersion, D^* (%)[b]	Exposed copper[a] (μmol Cu_S/g_{cat})
CZ	135.9 (5.7)	3.9	106.9 (4.4)
PCZ-CP	54.7 (2.3)	2.0	17.6 (0.7)
PCZ-SP	126.9 (5.3)	4.1	109.7 (4.5)

[a] The value in parentheses represents square meters of copper per gram of catalyst (m^2Cu/g_{cat}), assuming 1.46×10^{19} Cu atoms/m^2. The experimental error obtained by the frontal method was estimated to be lower than ±3%.

[b] Copper dispersion: D^* = exposed copper atoms/total copper atoms.

The copper dispersion, defined as the amount of exposed copper in relation to the total amount of copper atoms, is included in Table 4 for the reduced catalysts (third column). The low values seen for our systems in comparison with other literature examples (30) can be explained by the conditions applied during calcination. Fujita *et al.* (45) performed a detailed study into the effect of the calcination conditions on the final morphology, and hence on the catalytic performance for methanol synthesis, for Cu–Zn-based catalysts. They found that the calcination heating rate has a significant influence on the CuO crystallinity in samples obtained from aurichalcite decomposition. Specifically, the higher H_2O partial pressure resulting from the hydroxycarbonate decomposition at high heating rates (>10 K/min) causes the coalescence and growth of the CuO crystallites. Since we applied a heating rate of 10 K/min in the calcination step, the lower Cu dispersion obtained for the CZ and PCZ-SP catalysts (derived from aurichalcite decomposition) is explained by this relatively high heating rate.

Although the palladium loading in the modified catalysts is only about 2%, if all of this palladium were well dispersed (dispersion higher than 50%), then the Cu and Pd surface areas would be similar. In the absence of information about palladium dispersion, this rough approximation of the actual surface catalyst configuration leads us to reconsider the results for the modified system, especially for the PCZ-SP sample.

According to the points outlined in the preceding text, the true amount of exposed copper for the SP case should be lower than the value given in Table 4. However, if we compare all the characterisation results for CZ and PCZ-SP samples, both catalysts exhibit similar copper areas and also the CuO particle sizes were rather similar. This similarity between both catalysts leads us to believe that the difference between the real and estimated exposed copper in SP catalyst should not be too broad. Thus, the palladium dispersion of the PCZ-SP catalyst has to be small. The last point is consistent with the method of preparation. Palladium in the SP sample was added during the synthesis of the precursor. It is expected that a portion of the palladium added is encapsulated and kept within the bulk oxidic structures upon calcination.

Finally, in order to determine the extent of sintering during reaction, the amount of copper exposed after activity runs was measured after re-reduction of the sample. The postreaction values for exposed copper are shown in Table 4 (last column). Notable differences are apparent between the values for the fresh and postreaction catalysts. These differences range from a 15% decrease for PCZ-SP to almost 70% for PCZ-CP. This indicates that the thermal sintering of copper particles is an important factor during methanol synthesis with Cu–Zn-based catalysts. The loss of copper dispersion during reaction appears to be related to the rather low Hutting's temperature of copper (450 K, calculated as one-third of the melting temperature in kelvins),

i.e., the point at which the mobility of the copper atoms on the catalyst surface becomes significant. In this sense, most of the commercial catalysts, apart from a ZnO phase, also contain stabilizers such as Al_2O_3.

3.6. Catalytic Performance in Methanol Synthesis from CO_2/H_2

The hydrogenation of CO_2 mainly produced methanol, but the formation of CO took place simultaneously through the RWGS side reaction. The activities of the catalysts were fairly constant with time onstream and the reproducibility of the measurements was within ±7% of the mean value. C-containing products other than methanol and CO were not detected, except for some small fluctuating traces of methane at high temperatures. The selectivity is therefore defined as the ratio between the amount of CO_2 converted to MeOH and the amount of CO_2 converted to MeOH and CO. In any case, the carbon mass balance was more than acceptable (±5% difference between reactor input and output). The methanol yield (MTY), expressed as mole MeOH/(h kg_{cat}), is displayed as a function of reaction temperature in Fig. 4 (graph A). The methanol yield increases with increasing temperature, without any decreasing or limiting value, indicating that thermodynamic restrictions or diffusion limitations are absent. Although an exponential profile in the studied range of temperature is a preliminary proof of the lack of such restrictions, the change in the slope of the Arrhenius plot (observed reaction rate versus $1/T$) is more appropriate to detect external–internal diffusion limitations. Due to space restrictions, we can only advance that the values for the apparent activation energies obtained are within the values reported in the literature. So, the catalysts are working in the kinetic regime. CO production increases faster than the MTY with temperature, causing a decrease in the methanol selectivity with temperature and, therefore, with CO_2 conversion. This result is depicted in Fig. 4 (graph B), where the methanol selectivity decreases with CO_2 conversion.

The behavior of the catalysts containing palladium is very different. While the co-precipitated system PCZ-CP is almost inactive, the catalyst prepared by sequential precipitation (PCZ-SP) increases the MTY with respect to the CZ base catalyst. In order to rule out the possibility that the increase in the MTY is only due to an additive effect in which palladium is acting as an independent catalytic site, a reference catalyst (2/98 wt% PdO–ZnO) was prepared by the sequential precipitation method. The absence of activity for this catalyst indicates that palladium, in the PCZ-SP catalyst, does not act as an independent and additional catalytic site for methanol synthesis but gives rise to a synergetic effect. Given that the selectivity towards MeOH for the same CO_2 conversion was higher for the PCZ-SP catalyst than CZ (Fig. 4, graph B), it is clear that the enhancement in MTY is due to an increase in the selectivity

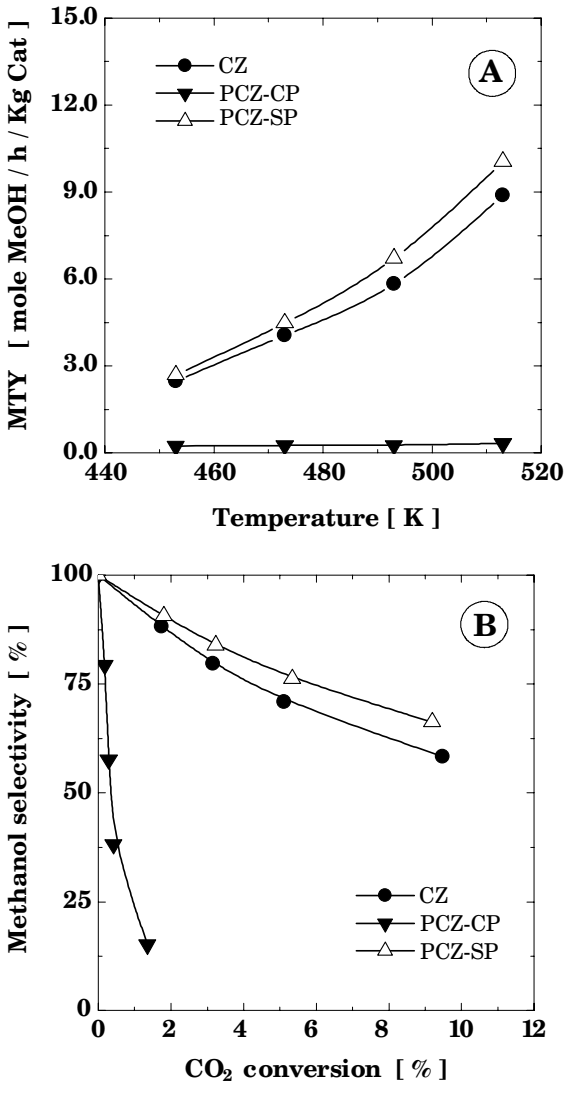

FIG. 4. (A) Methanol yield [mol MeOH/(h kg_{cat})] as a function of the reaction temperature for the catalysts; (B) methanol selectivity against CO_2 conversion. Conditions: $P = 60$ bar, $CO_2/H_2 = 3$, $W/F = 0.0675$ kg h/m^3 and $T = 453$–513 K.

and not in the CO_2 conversion. Therefore, the active centers are more selective for methanol synthesis. This finding is also consistent with the fact that the rate-determining step for methanol synthesis involves the hydrogenolysis of adsorbed dioximethane (H_2COO^*), a situation where palladium would exert its hydrogenating role, whereas the RWGS side reaction involves a nonhydrogenation step as the rate-limiting step, namely the dissociation of adsorbed water to OH^* and H^*.

4. DISCUSSION

Structure–activity relationship. An optimal method to introduce palladium into a conventional CuO–ZnO methanol synthesis catalyst should not decrease the copper

phase dispersion. Although the existing models for the active centers that participate in the methanol synthesis show discrepancies regarding the final role of ZnO (46–52), all of them confirm the importance of metallic copper. Copper is required to be highly dispersed and any decrease in copper dispersion would cause a lowering of activity. Thus, the aforementioned decrease in the catalytic activity of the PCZ-CP catalyst can be interpreted in terms of loss of copper surface area, as revealed by the N_2O chemisorption measurements. This poor copper dispersion for PCZ-CP is a consequence of two combined effects: the formation of the oxidic phases from the decomposition of independent Cu and Zn phases in the precursor (30) and the high level of residual Na after calcination. Both factors inhibit the interaction between CuO and ZnO and result in an increase in the particle size of both oxidic phases. The TPR experiment shows a concomitant result in terms of the increased difficulty of CuO reduction (wide reduction peak) as a consequence of the large CuO crystallites. The loss of interaction between Cu and Zn oxides not only leads to a low Cu dispersion in the reduced state, but also to a decrease in the thermal stability during reaction, as revealed by the N_2O chemisorption measurement after reaction. In addition, the TPR technique proves the low degree of interaction between Pd and Cu–Zn since the Pd phase is reduced as isolated and large PdO particles. This catalyst configuration involving separate and weakly interacting Pd, Cu, and Zn phases, which is obtained by co-precipitation, creates a situation in which the effect of palladium is not capable of overcoming the loss in copper surface area.

The incorporation of palladium by the sequential precipitation methodology improves the methanol performance of the PCZ-SP catalyst for the direct hydrogenation of CO_2, as compared to the base CZ material. This enhancement is not due to additional active palladium sites, but to a synergetic effect of Pd on the active Cu sites. At the calcined level, the oxide phases are formed by decomposition of an aurichalcite phase (25). This structure, in which Cu and Zn are atomically dispersed in a hydroxycarbonate matrix, gives rise to well-interdispersed oxide phases similar to those already found for the CZ precursor. In the reduced state, the copper surface area for the H_2-reduced PCZ-SP catalyst is almost the same as for the CZ sample. Therefore, it is clear that the enhancement in the MTY for PCZ-SP cannot be explained simply by a modification of the copper dispersion associated with the incorporation of Pd. However, the fact that the copper dispersion is maintained in a similar way to the base CZ material is a key factor in the preparation of an optimised Pd-modified system. Thus, the good results obtained for the sequential precipitation methodology arise because the aurichalcite precursor structure is maintained upon palladium addition; the copper dispersion is maintained at the same level as in the CZ catalyst and the effect of palladium is manifested.

TPR and XPS experiments were very helpful in clarifying the promoting effect of palladium in the PCZ-SP catalyst: an enhancement in CuO reducibility and an increase in the hydrogen consumption are evident. The increase in the amount of hydrogen consumed (H_2/M) during CuO reduction for PCZ-SP, with respect to the CZ counterpart, indicates that hydrogen is easily dissociated on Pd particles and then spilled over the Cu–ZnO phase. Furthermore, an enhancement in the CuO reducibility was observed by TPR and supported by XPS. Such a reducibility effect for Pd-containing CuO–ZnO-based catalysts has scarcely been reported in the literature but is generally interpreted as being due to a direct interaction between Pd and Cu. The good interaction between Pd and Cu means that the H_2 spillover becomes effective in terms of improvement of CuO reducibility and, consequently, it is expected to show an enhancement in the performance for methanol synthesis, as indeed is observed. However, other different mechanisms of promotion on the working Pd-modified catalysts cannot be ruled out. We recently proposed a novel mechanism in which Pd, either by an "ensemble" or "ligand effect," modifies the surface redox properties of Cu (53). Therefore, it is reasonable to think that several mechanisms are performing during reaction.

The hypothesis of an H_2-spillover mechanism as responsible for the increase in the MTY was also proposed by Inui and Takeguchi (16) and Sahibzada *et al.* (18), who reported that H_2 spillover influences the transportation rate of hydrogen to the active centers. Moreover, this mechanism keeps the copper surface in a more reduced state, thus counteracting the oxidising effect of the CO_2 and/or water by-product. As far as the PCZ-CP catalyst is concerned, the higher (H_2/M) ratio obtained for this catalyst suggests that the spillover effect of palladium is occurring, but becomes ineffective during the synthesis of methanol due to the low copper surface area. The effect of palladium is not capable of overcoming this large loss of exposed copper. In fact, palladium cannot enhance the reducibility of CuO due to the large dimensions of the CuO particles.

In summary, the structure–activity relationship reveals the importance of the method of palladium incorporation and clearly demonstrates that the precipitation order has a remarkable influence on the properties of the active phases and, therefore, on the catalytic performance for the hydrogenation of CO_2 to methanol.

5. CONCLUSIONS

Variation of the palladium incorporation methodology, i.e., co-precipitation (PCZ-CP) versus sequential precipitation (PCZ-SP), has a remarkable effect on the catalytic performance for the hydrogenation of CO_2 to methanol. The decrease in the MTY for PCZ-CP is accompanied by significant changes in bulk and surface properties of the

catalyst, i.e., large CuO particle sizes, very low copper surface area, difficulty in CuO reduction, and greater instability towards sintering. These features are due to the fact that the PCZ-CP catalyst is obtained from calcination of two separate Cu and Zn precursor phases (sodium–zinc carbonate and an amorphous copper hydroxycarbonate) and from the high loading of residual Na in the calcined catalyst. Both of these factors inhibit the interaction between CuO and ZnO phases, leading to a poor copper dispersion in the reduced state. The effect of palladium is not capable of overcoming the loss in copper surface area.

On the other hand, the addition of Pd in the PCZ-SP catalyst results in a synergetic effect of Pd on the active Cu sites. The increase in the amount of hydrogen consumed (H_2/M) of this catalyst during CuO reduction points to the H_2-spillover mechanism as being responsible for the increase in the methanol yield. Moreover, the possibility that several mechanisms are performing during reaction cannot be ruled out. It appears that sequential precipitation is a suitable method to introduce palladium. The use of this method maintains the copper dispersion at the same level as the reference CZ catalyst—by keeping the aurichalcite precursor structure upon palladium addition—and the promoting effect of the palladium clearly emerges during reaction.

ACKNOWLEDGMENT

This work was supported by CICYT (Spain) under Grant QUI98–0877. I. Melián-Cabrera thanks the Ministry of Education and Science for a fellowship.

REFERENCES

1. Chinchen, G. C., Mansfield, K., and Spencer, M. S., *CHEMTECH* **Nov**, 692 (1990).
2. Kagan, Y. B., Liberov, L. G., Slivinskii, E. V., Loktev, S. M., Lin, G. I., Rozovskii, A. Y., and Bashkirov, A. N., *Dokl. Akad. Nauk SSSR* **221**, 1093 (1975).
3. Chinchen, G. C., Denny, P. J., Parker, D. G., and Spencer, M. S., *Appl. Catal.* **30**, 333 (1987).
4. Bowker, M., Hadden, R. A., Houghton, H., Hyland, J. N. K., and Waugh, K. C., *J. Catal.* **109**, 263 (1988).
5. Inui, T., Hara, H., Takeguchi, T., and Kim, J. B., *Catal. Today* **36**, 25 (1997).
6. Saito, M., Fujitani, T., Takeuchi, M., and Watanabe, T., *Appl. Catal., A* **138**, 311 (1996).
7. Tagawa, T., Pleizier, G., and Amenomiya, Y., *Appl. Catal.* **18**, 285 (1985).
8. Amenomiya, Y., *Appl. Catal.* **30**, 57 (1987).
9. Koeppel, R. A., Baiker, A., Schild, C., and Wokaun, W., *Stud. Surf. Sci. Catal.* **63**, 59 (1991).
10. Kanoun, N., Astier, M. P., and Pajonk, G. M., *Catal. Lett.* **15**, 231 (1992).
11. Walker, A. P., Lambert, R. M., Nix, R. M., and Jennings, J. R., *J. Catal.* **138**, 694 (1992).
12. Barrault, J., Rassoul, Z., and Bettahar, M. M., *Stud. Surf. Sci. Catal.* **61**, 367 (1991).
13. Arakawa, H., Sayama, K., Okabe, K., and Murakami, A., *Stud. Surf. Sci. Catal.* **77**, 389 (1993).
14. Fujitani, T., Saito, M., Kanai, Y., Kakumoto, T., Watanabe, T., Nakamura, J., and Uchijima, T., *Catal. Lett.* **25**, 271 (1994).
15. Toyir, J., de la Piscina, P. R., Fierro, J. L. G., and Homs, N., *Appl. Catal., B* **29**, 207 (2001).
16. Inui, T., and Takeguchi, T., *Catal. Today* **10**, 95 (1991).
17. Fujimoto, K., and Yu, Y., *Stud. Surf. Sci. Catal.* **77**, 393 (1993).
18. Sahibzada, M., Chadwick, D., and Metcalfe, I. S., *Catal. Today* **29**, 367 (1996).
19. Gotti, A., and Prins, R., *J. Catal.* **175**, 302 (1998).
20. Melián-Cabrera, I., López Granados, M., Terreros, P., and Fierro, J. L. G., *Catal. Today* **45**, 251 (1998).
21. Melián-Cabrera, I., López Granados, M., and Fierro, J. L. G., *J. Catal* **210**, 273 (2002).
22. Geus, J. W., and van Veen, J. A. R., *Stud. Surf. Sci. Catal.* **123**, 459 (1999).
23. Cavani, F., Trifirò, F., and Vaccari, A., *Catal. Today* **11**, 173 (1991).
24. Vaccari, A., *Appl. Clay Sci.* **14**, 161 (1999).
25. Melián-Cabrera, I., López Granados, M., and Fierro, J. L. G., *Chem. Mater.* **14**, 1863 (2002).
26. Herman, R. G., Klier, K., Simmons, G. W., Finn, B. P., Bulko, J. B., and Kobylinski, T. P., *J. Catal.* **56**, 407 (1979).
27. Spencer, M. S., *Top. Catal.* **8**, 259 (1999).
28. Shen, G. C., Fujita, S., Matsumoto, S., and Takezawa, N., *J. Mol. Catal. A: Chemical* **124**, 123 (1997).
29. Chinchen, G. C., Hay, C. M., Vandervell, H. D., and Waugh, K. C., *J. Catal.* **103**, 79 (1987).
30. Dell, R. M., Stone, F. S., and Tiley, P. F., *Trans. Faraday Soc.* **49**, 195 (1953).
31. Jun, K. W., Shen, W. J., Rao, K. S. R., and Lee, K. W., *Appl. Catal., A* **174**, 231 (1998).
32. Fierro, G., Lo Jacono, M., Inversi, M., Porta, P., Cioci, F., and Lavecchia, R., *Appl. Catal., A* **137**, 327 (1996).
33. Fleisch, T. H., and Mieville, R. L., *J. Catal.* **90**, 165 (1984).
34. Boyce, A. L., Sermon, P. A., Vong, M. S. W., and Yates, M. A., *React. Kinet. Catal. Lett.* **44**, 309 (1991).
35. Waugh, K. C., *Catal. Today* **15**, 51 (1992).
36. Bailey, S., and Waugh, K. C., *Catal. Lett.* **17**, 371 (1993).
37. Chang, T. C., Chen, J. J., and Yeh, C. T., *J. Catal.* **96**, 51 (1985).
38. Jones, A., and McNicol, B. D., "Temperature-Programmed Reduction for Solid Materials Characterization." Dekker, New York, 1986.
39. Kissinger, H. E., *Anal. Chem.* **29**, 1702 (1957).
40. Gentry, S. J., Hurst, N. W., and Jones, A., *J. Chem. Soc., Faraday Trans. 1* **77**, 603 (1981).
41. Okamoto, Y., Fukino, K., Imanaka, T., and Teranishi, S., *J. Phys. Chem.* **87**, 3740 (1983).
42. Porta, P., Campa, M. C., Fierro, G., Lo Jacono, M., Minelli, G., Moretti, G., and Stoppa, L., *J. Mater. Chem.* **3**, 505 (1993).
43. Wagner, C. D., and Joshi, A., *J. Electron Spectrosc. Relat. Phenom.* **47**, 283 (1988).
44. Fierro, J. L. G., *Catal. Rev.—Sci. Eng.* **34**, 255 (1993).
45. Fujita, S., Moribe, S., Kanamori, Y., Kakudate, M., and Takezawa, N., *Appl. Catal., A* **207**, 121 (2001).
46. Spencer, M. S., *Catal. Lett.* **50**, 37 (1998).
47. Fujitani, T., and Nakamura, J., *Catal. Lett.* **56**, 119 (1998).
48. Spencer, M. S., *Top. Catal.* **8**, 259 (1999).
49. Waugh, K. C., *Catal. Lett.* **58**, 163 (1999).
50. Spencer, M. S., *Catal. Lett.* **66**, 255 (2000).
51. Grunwaldt, J. D., Molenbroek, A. M., Topsøe, N. Y., Topsøe, H., and Clausen, B. S., *J. Catal.* **194**, 452 (2000), doi:10.1006/jcat.2000.2930.
52. Choi, Y., Futagami, K., Fujitani, T., and Nakamura, J., *Appl. Catal., A* **208**, 163 (2001).
53. Melián-Cabrera, I., López Granados, M., and Fierro, J. L. G., *Catal. Lett.* **79**, 165 (2002).